Mon. Not. R. Astron. Soc. **000**, 1–12 (2010) Printed 8 September 2010 (MN LATEX style file v2.2)

Two years of monitoring Supergiant Fast X–ray Transients with *Swift*

P. Romano[1], V. La Parola[1], S. Vercellone[1], G. Cusumano[1], L. Sidoli[2], H.A. Krimm[3,4], C. Pagani[5,6], P. Esposito[7,8], E.A. Hoversten[5], J.A. Kennea[5], K.L. Page[6], D.N. Burrows[5], N. Gehrels[4]

[1]*INAF, Istituto di Astrofisica Spaziale e Fisica Cosmica, Via U. La Malfa 153, I-90146 Palermo, Italy*
[2]*INAF, Istituto di Astrofisica Spaziale e Fisica Cosmica, Via E. Bassini 15, I-20133 Milano, Italy*
[3]*NASA/Goddard Space Flight Center, Greenbelt, MD 20771, USA*
[4]*Universities Space Research Association, Columbia, MD, USA*
[5]*Department of Astronomy and Astrophysics, Pennsylvania State University, University Park, PA 16802, USA*
[6]*Department of Physics & Astronomy, University of Leicester, LE1 7RH, UK*
[7]*INAF, Osservatorio Astronomico di Cagliari, località Poggio dei Pini, strada 54, I-09012 Capoterra, Italy*
[8]*Istituto Nazionale di Fisica Nucleare, sezione di Pavia, via A. Bassi 6, I-27100 Pavia, Italy*

arXiv:1009.1146v1 [astro-ph.HE] 6 Sep 2010

Accepted 2010 August 18. Received 2010 August 17; in original form 2010 March 17

ABSTRACT

We present results based on two years of intense *Swift* monitoring of three supergiant fast X–ray transients (SFXTs), IGR J16479−4514, XTE J1739−302, and IGR J17544−2619, which we started in October 2007. Our out-of-outburst intensity-based X–ray (0.3–10 keV) spectroscopy yields absorbed power laws characterized by hard photon indices ($\Gamma\sim$1–2). The broad-band (0.3–150 keV) spectra of these sources, obtained while they were undergoing new outbursts observed during the second year of monitoring, can be fit well with models typically used to describe the X–ray emission from accreting neutron stars in high-mass X–ray binaries. We obtain an assessment of how long each source spends in each state using a systematic monitoring with a sensitive instrument. By considering our monitoring as a casual sampling of the X–ray light curves, we can infer that the time these sources spend in bright outbursts is between 3 and 5 % of the total. The most probable X-ray flux for these sources is $\sim$ 1–2 $\times$ 10^{-11} erg cm^{-2} s^{-1} (2–10 keV, unabsorbed), corresponding to luminosities in the order of a few 10^{33} to a few 10^{34} erg s^{-1} (two orders of magnitude lower than the bright outbursts). In particular, the duty-cycle of *inactivity* is $\sim 19, 39, 55$ % (~ 5 % uncertainty), for IGR J16479−4514, XTE J1739−302, and IGR J17544−2619, respectively. We present a complete list of BAT on-board detections, which further confirms the continued activity of these sources. This demonstrates that true quiescence is a rare state, and that these transients accrete matter throughout their life at different rates. Variability in the X–ray flux is observed at all timescales and intensity ranges we can probe. Superimposed on the day-to-day variability is intra-day flaring which involves flux variations up to one order of magnitude that can occur down to timescales as short as $\sim$ 1 ks, and which can be naturally explained by the accretion of single clumps composing the donor wind with masses $M_{\rm cl} \sim 0.3$–2×10^{19} g. Thanks to the *Swift* observations, the general picture we obtain is that, despite individual differences, common X–ray characteristics of this class are now well defined, such as outburst lengths well in excess of hours, with a multiple peaked structure, and a high dynamic range (including bright outbursts), up to ~ 4 orders of magnitude.

Key words: X-rays: binaries – X-rays: individual: IGR J16479−4514, XTE J1739−302, IGR J17544−2619.
Facility: *Swift*

1 INTRODUCTION

Supergiant fast X–ray transients (SFXTs) constitute a new class of High Mass X–ray Binaries (HMXBs). Discovered by *INTE-*

Table 4. Summary of the *Swift*/XRT monitoring campaign.

Name	Campaign Start (yyyy-mm-dd)	Campaign End (yyyy-mm-dd)	N[a]	Exposure[b] (ks)	Outburst[c] Dates (yyyy-mm-dd)	BAT Trigger	References
IGR J16479−4514	*2007-10-26*	*2008-10-25*	*70*	*75.2*	*2008-03-19*	*306829*	*Romano et al. (2008d)*
					2008-05-21	*312068*	
	2009-01-29	2009-10-25	74	85.7	2009-01-29	341452	Romano et al. (2009e); La Parola et al. (2009)
XTE J1739−302	*2007-10-27*	*2008-10-31*	*95*	*116.1*	*2008-04-08*	*308797*	*Romano et al. (2008c); Sidoli et al. (2009c)*
					2008-08-13	*319963*	*Romano et al. (2008b), Sidoli et al. (2009a)*
	2009-02-21	2009-11-01	89	89.6	2009-03-10	346069	Romano et al. (2009d), this work
IGR J17544−2619	*2007-10-28*	*2008-10-31*	*77*	*74.8*	*2007-11-08*	BTM	*Krimm et al. (2007)*
					2008-03-31	*308224*	*Sidoli et al. (2008a, 2009c)*
					2008-09-04	XM	*Romano et al. (2008a); Sidoli et al. (2009a)*
	2009-02-21	2009-11-03	65	68.0	2009-03-15	BTM	Krimm et al. (2009)
					2009-06-06	354221	Romano et al. (2009f)
First year			*330*	*362.6*			
Second year			228	243.3			
Total			558	605.9			

[a] Number of observations (individual OBSIDs) obtained during the monitoring campaign.

[b] *Swift*/XRT net exposure.

[c] BAT trigger dates. BTM=triggered the BAT Transient Monitor; XM=discovered in XRT monitoring data.

Note. We report the data from the first year in italics.

GRAL (Sguera et al. 2005), they are firmly associated with OB supergiant stars via optical spectroscopy, and display sporadic X–ray outbursts significantly shorter than those of typical Be/X–ray binaries, characterized (as observed by *INTEGRAL*/IBIS) by bright flares (peak luminosities of 10^{36}–10^{37} erg s^{-1}) lasting a few hours (Sguera et al. 2005; Negueruela et al. 2006). The quiescence, which is characterized by a soft spectrum (likely thermal) shows a luminosity of $\sim 10^{32}$ erg s^{-1} so that SFXTs display a dynamic range of 3–5 orders of magnitude. Their hard X–ray spectra during outburst resemble those of HMXBs hosting accreting neutron stars, with hard power laws below 10 keV combined with high energy cut-offs at $\sim$ 15–30 keV, sometimes strongly absorbed at soft energies (Walter et al. 2006; Sidoli et al. 2006). Therefore, it is tempting to assume that all SFXTs might host a neutron star, even if pulse periods have only been measured for a few SFXTs. Consensus has not been reached yet on the actual mechanism producing the outbursts, but it is probably related to either the properties of the wind from the supergiant companion (in't Zand 2005; Walter & Zurita Heras 2007; Negueruela et al. 2008; Sidoli et al. 2007) or the presence of gated mechanisms (Bozzo et al. 2008).

Swift is currently the only observatory which, thanks to its unique fast-slewing capability and its broad-band energy coverage, can catch outbursts from these fast transients in their very early stages and study them panchromatically as they evolve, thus providing invaluable information on the nature of the mechanisms producing them.

Furthermore, thanks to its flexible observing scheduling, which makes a monitoring effort cost-effective, *Swift* has given SFXTs the first non serendipitous attention through monitoring campaigns that cover all phases of their lives with a high sensitivity in the soft X–ray regime, where most SFXTs had not been observed before (Romano et al. 2009b).

In our previous papers of this series, we described the long-term X–ray emission outside the bright outbursts based on the first 4 months of data (Sidoli et al. 2008b, Paper I); the outbursts of IGR J16479−4514 (Romano et al. 2008d, Paper II; Romano et al. 2009b, Paper V); and the prototypical IGR J17544−2619 and XTE J17391−302 (Sidoli et al. 2009c, Paper III; Sidoli et al. 2009a, Paper IV).

In this paper we continue our characterization of the long term properties of our sample as derived from a two-year-long high-sensitivity X–ray coverage. We report on the new X–ray Telescope (XRT, Burrows et al. 2005) and the UV/Optical Telescope (UVOT, Roming et al. 2005) data collected in 2009 between January 29 and November 3 and we exploit the longer baseline for in-depth soft X–ray spectral analysis. Furthermore, we show our results on the outbursts caught by the Burst Alert Telescope (BAT, Barthelmy et al. 2005) during the second year of our monitoring campaign, as well as the BAT on-board triggers registered during 2009.

2 SAMPLE AND OBSERVATIONS

During the second year of *Swift* observations, we monitored three targets, XTE J1739–302, IGR J17544−2619, and IGR J16479−4514.

XTE J1739−302 was discovered in August 1997 by *RXTE* (Smith et al. 1998), when it reached a peak flux of 3.6×10^{-9} erg cm^{-2} s^{-1} (2–25 keV) and has a long history of flaring activity recorded by *INTEGRAL* (Sguera et al. 2006; Walter & Zurita Heras 2007; Blay et al. 2008) and by *Swift* (Sidoli et al. 2009c,a). Recently, Drave et al. (2010) reported the discovery of a 51.47 ± 0.02 d orbital period based on ~ 12.4 Ms of *INTEGRAL* data. The optical counterpart is an O8I star (Negueruela et al. 2006).

The first recorded flare from IGR J17544−2619 was observed by *INTEGRAL* in 2003 (Sunyaev et al. 2003), when the source reached a flux of 160 mCrab (18–25 keV). Several more

flares, lasting up to 10 hours, were detected by *INTEGRAL* in the following years (Grebenev et al. 2003, 2004; Sguera et al. 2006; Walter & Zurita Heras 2007; Kuulkers et al. 2007) with fluxes up to 400 mCrab (20–40 keV) and some were found in archival *BeppoSAX* observations (in't Zand et al. 2004). Subsequent flares were observed by *Swift* (Krimm et al. 2007; Sidoli et al. 2009c,a), and *Suzaku* (Rampy et al. 2009). Recently, Clark et al. (2009) reported the discovery of a 4.926 ± 0.0001 d orbital period based on the ~ 4.5 years of *INTEGRAL* data. The optical counterpart is an O9Ib star (Pellizza et al. 2006).

IGR J16479−4514 was discovered by *INTEGRAL* in 2003 (Molkov et al. 2003), during an outburst that reached the flux level of $\sim$ 12 mCrab (18–25 keV). Since then the source has shown frequent flaring activity, recorded by both *INTEGRAL* (Sguera et al. 2005, 2006; Walter & Zurita Heras 2007) and *Swift* (Kennea et al. 2005; Markwardt & Krimm 2006; Romano et al. 2008d; Bozzo et al. 2009; Romano et al. 2009b), which led to its inclusion in the SFXT class. The optical counterpart is an O8.5I star (Rahoui et al. 2008). Recently, Bozzo et al. (2008) reported an episode of sudden obscuration in a long *XMM–Newton* observation obtained after the 2009 March 19 outburst, possibly an X–ray eclipse by the supergiant companion. This was later confirmed by Jain et al. (2009), who discovered a 3.32 d orbital period in the first 4 years of BAT data and *RXTE*/ASM data, and by Romano et al. (2009b) by using XRT observations covering one year.

We monitored the first two targets as they are generally considered prototypical SFXTs, and the latter because of its frequent triggering of the BAT since the beginning of the mission. We planned two observations week^{-1} object^{-1} (IGR J16479−4514 and IGR J17544−2619) and 3 observations week^{-1} object^{-1} (XTE J1739–302), each 1 ks long. The observation logs are reported in Tables 1, 2, and 3. This strategy was chosen to fit within the regular observing schedule of the main observing targets for *Swift*, γ-ray bursts (GRBs). Furthermore, in order to ensure simultaneous narrow field instrument (NFI) data, the *Swift* Team enabled automatic rapid slews to these objects following detection of flares by the BAT, in the same fashion as is currently done for GRBs. During the campaign we often requested target of opportunity (ToO) observations whenever one of the sources showed interesting activity, or following outbursts to better monitor the decay of the XRT light curve, thus obtaining a finer sampling of the light curves and allowing us to study all phases of the evolution of an outburst.

During the second year (2009), we collected a total of 228 *Swift* observations as part of our program, for a total net XRT exposure of $\sim$ 243 ks accumulated on all sources and distributed as shown in Table 4.

3 DATA REDUCTION

The XRT data were uniformly processed with standard procedures (XRTPIPELINE v0.12.3), filtering and screening criteria by using FTOOLS in the HEASOFT package (v.6.7). We considered both windowed-timing (WT) and photon-counting (PC) mode data, and selected event grades 0–2 and 0–12, respectively (Burrows et al. 2005). When appropriate, we corrected for pile-up by determining the size of the affected core of the point spread function (PSF) by comparing the observed and nominal PSF (Vaughan et al. 2006), and excluding from the analysis all the events that fell within that region. We used the latest spectral redistribution matrices in CALDB (20091130).

The BAT data of the outbursts (see Sect. 5) were analysed using the standard BAT software within FTOOLS. Mask-tagged BAT light curves were created in the standard energy bands, and rebinned to fulfil at least one of the following conditions, achieving a signal-to-noise (S/N) of 5 or bin length of 100 s. Response matrices were generated with BATDRMGEN using the latest spectral redistribution matrices. For this paper we also considered the BAT Transient Monitor data (Krimm et al. 2006, 2008)[1], covering the same time interval as the NFI pointed observations. The data were rebinned to a 4 d resolution to ensure a larger number of detections and to closely match the NFI sampling.

The UVOT observed the 3 targets simultaneously with the XRT. The data of XTE J1739−302 and IGR J16479−4514 were taken in general with the 'Filter of the Day' (FoD), i.e. the filter chosen for all observations to be carried out during a specific day in order to minimize the filter wheel rotation (u, $uvw1$, $uvw2$ and $uvm2$), while IGR J17544−2619 was only observed with UVOT from 2009-06-06 to 2009-09-30, in the $uvw1$ and v filters, and in FoD for the remainder of the campaign. However, during the outbursts of 2009-03-10 of XTE J1739−302 and 2009-06-06 of IGR J17544−2619 all filters were used in the typical GRB sequence (Roming et al. 2005). The data analysis was performed using the UVOTIMSUM and UVOTSOURCE tasks included in the FTOOLS software. The latter task calculates the magnitude through aperture photometry within a circular region and applies specific corrections due to the detector characteristics. The reported magnitudes are on the UVOT photometric system described in Poole et al. (2008), and are not corrected for Galactic extinction. At the position of IGR J16479−4514, no detection was achieved down to a 3σ limit of $u = 21.27$ mag.

All quoted uncertainties are given at 90 % confidence level for one interesting parameter unless otherwise stated. The spectral indices are parameterized as $F_\nu \propto \nu^{-\alpha}$, where F_ν (erg cm^{-2} s^{-1} Hz^{-1}) is the flux density as a function of frequency ν; we adopt $\Gamma = \alpha + 1$ as the photon index, $N(E) \propto E^{-\Gamma}$ (ph cm^{-2} s^{-1} keV^{-1}).

4 TIMING

4.1 XRT light curves and inactivity duty cycle

The 0.2–10 keV XRT light curves collected from 2007 October 26 to 2009 November 3, are shown in Fig. 1. They are corrected for pile-up, PSF losses, and vignetting, and background-subtracted. Each point in the light curves refers to the average flux observed during each observation performed with XRT; the exceptions are the outbursts (listed in Table 4) where the data were binned to include at least 20 source counts per time bin to best represent the count rate dynamical range.

One of our goals is to calculate the percentage of time each source spent in each flux state. We consider our monitoring as a casual sampling of the light curve at a resolution of $\sim$ 3–4 d over a $>$ 2 yr baseline. We considered the following three states, *i)* BAT-detected outburst, *ii)* intermediate state (all observations yielding a firm detection excluding outburst ones), *iii)* 'non detections' (detections with a significance below 3σ). From the latter state we excluded all observations that had a net exposure below 900 s [corresponding to 2–10 keV flux limits that vary between 1 and 3×10^{-12} erg cm^{-2} s^{-1} (3σ), depending on the source, see Romano et al. (2009b)]. This was done because *Swift* is a GRB-chasing mission

[1] http://swift.gsfc.nasa.gov/docs/swift/results/transients/

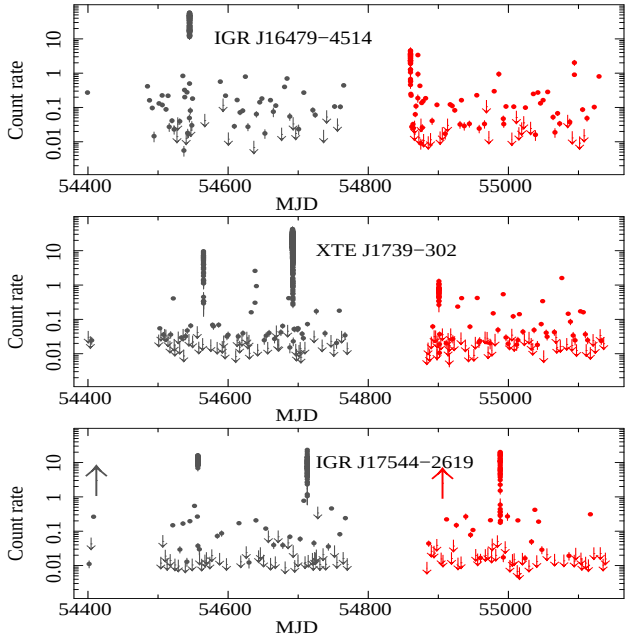


Figure 1. *Swift*/XRT (0.2–10 keV) light curves. The data were collected from 2007 October 26 to 2008 November 15 (first year, grey) and from 2009 January 29 to November 3 (second year, red). The downward-pointing arrows are 3σ upper limits. The upward pointing arrows mark flares that triggered the BAT Transient Monitor on MJD 54414 and 54906. Data up to MJD ~ 54770 (grey) were published in Romano et al. (2009b).

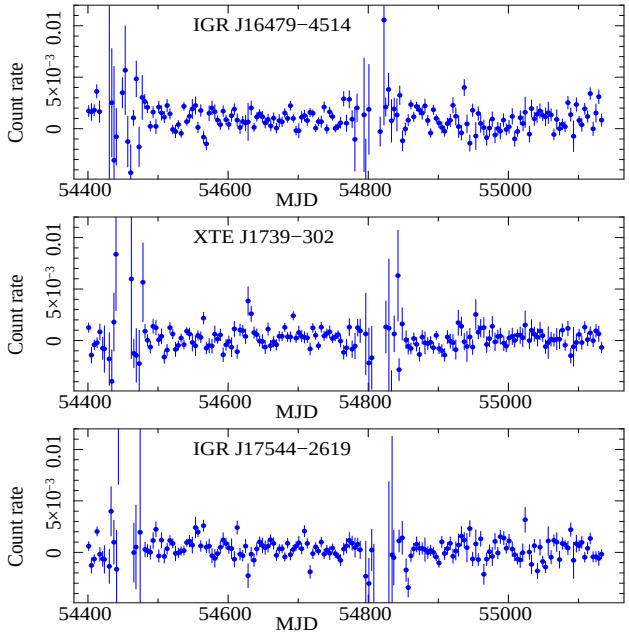


Figure 2. *Swift*/BAT Transient Monitor light curves in the 15–50 keV energy range in units of counts s^{-1} cm^{-2}.

Table 5. Duty cycle of inactivity of the three SFXTs (2-year campaign).

Name	ΔT_Σ (ks)	$P_{\rm short}$ (%)	IDC (%)	Rate$_{\Delta T_\Sigma}$ (10^{-3}counts s^{-1})
IGR J16479−4514	29.7	3	19	3.1 ± 0.5
XTE J1739−302	71.5	10	39	4.0 ± 0.3
IGR J17544−2619	69.3	10	55	2.2 ± 0.2

Count rates are in units of 10^{-3} counts s^{-1} in the 0.2–10 keV energy band. ΔT_Σ is sum of the exposures accumulated in all observations, each in excess of 900 s, where only a 3σ upper limit was achieved; $P_{\rm short}$ is the percentage of time lost to short observations; IDC is the duty cycle of *inactivity*, *i.e.,* the time each source spends undetected down to a flux limit of 1–3$\times 10^{-12}$ erg cm^{-2} s^{-1}; Rate$_{\Delta T_\Sigma}$ is detailed in the text (Sect. 4.1).

and several observations were interrupted by GRB events; therefore the consequent non detection may be due to the short exposure, and not exclusively to the source being faint.

The duty cycle of *inactivity* is defined (Romano et al. 2009b) as the time each source spends *undetected* down to a flux limit of 1–3$\times 10^{-12}$ erg cm^{-2} s^{-1},

$$\mathrm{IDC} = \Delta T_\Sigma / [\Delta T_{\rm tot}\,(1 - P_{\rm short})]\,, \quad (1)$$

where ΔT_Σ is sum of the exposures accumulated in all observations, each in excess of 900 s, where only a 3σ upper limit was achieved (Table 5, column 2), $\Delta T_{\rm tot}$ is the total exposure accumulated (Table 4, column 5), and $P_{\rm short}$ is the percentage of time lost to short observations (exposure $<$ 900 s, Table 5, column 2). We obtain that IDC $= 19, 39, 55$ %, for IGR J16479−4514, XTE J1739–302, and IGR J17544−2619, respectively (Table 5, column 3), with an estimated error of ~ 5 %. We note that these values are based on the whole 2-year campaign, and that the IDC calculated with the observations of 2009 only is $21, 39, 55$ %. Finally, as we can consider our monitoring as a casual sampling of the light curve, we can also infer that the time these sources spend in bright outbursts is between 3 and 5 % of the total (estimated error of ~ 5 %).

4.2 BAT transient monitor data and on-board detections

The 15–50 keV BAT Transient Monitor light curves collected from 2007 October 26 to 2009 November 3, are shown in Fig. 2, rebinned at a 4 d resolution. The two gaps in each of the BAT light curves preceded and followed by points with large error bars are an artifact of *Swift*'s Sun-avoidance pointing strategy. When the sources are near the Sun, they will be found only at the edges of the BAT FOV, where the sensitivity is reduced and for a few weeks each year the sources cannot be observed at all.

In Table 6 we report the BAT on-board detections in the 15–50 keV band. If an alert was generated, a BAT trigger was assigned (Column 4) and notices were disseminated[2]. For some of these triggers a burst response (slew and repointing of the NFI) was also initiated, depending on GRB observing load, observing constraints, and interest in the sources. More details on several of these triggers can be found in the papers of our series (see Table 4, for references). The combination of all these data show how active the sources are outside the bright outbursts when observed by the BAT.

[2] http://gcn.gsfc.nasa.gov/gcn/swift_grbs.html

Table 6. BAT on-board detections in the 15–50 keV band during 2009.

MJD	Date	Time[a]	BAT Trigger N.[b]	S/N[c]
		IGR J16479−4514		
54860	2009-01-29	06:32:06–06:48:1	341452 (NFI)	10.68
54895	2009-03-04	17:43:07–18:13:47		
54915	2009-03-25	00:13:07		
54958	2009-05-06	19:06:51		
54986	2009-06-03	23:45:07		
55079	2009-09-05	00:09:35		
55116	2009-10-12	03:25:31–03:47:39		
		XTE J1739−302		
54901	2009-03-10	18:18:35–18:45:15	346069 (NFI)[d]	6.81
55079	2009-09-05	05:00:27		
55107	2009-10-03	01:07:15-01:16:51		
		IGR J17544−2619		
54945	2009-04-24	11:19:15		
54988	2009-06-06	07:49:00	354221 (NFI)[e]	8.15
55002	2009-06-20	02:45:39		
55024	2009-07-12	10:59:55		
55063	2009-08-20	03:16:43		
55074	2009-08-30	12:33:55		
55132	2009-10-28	19:24:11		

[a] Time of the start of the BAT trigger, or the time range when on-board detections were obtained.

[b] BAT regular trigger, as was disseminated through GCNs. NFI indicates that there are data from the narrow-field instrument.

[c] On-board image significance in units of σ.

[d] This work, Sect 5.1.

[e] This work, Sect 5.2.

4.3 UVOT light curves

The UVOT performed observations simultaneously with the XRT, throughout most of the *Swift*/XRT monitoring of the SFXTs. Figure 3a,b shows the UVOT u and $uvw1$ light curves of XTE J1739−302 of the whole campaign. The dashed vertical lines mark the X–ray outbursts. The u and $uvw1$ magnitudes show variability of marginal statistical significance; a fit against a constant yields $\chi^2_\nu(u) = 2.13$ for 45 degrees of freedom (dof), null hypothesis probability nhp$= 1.5 \times 10^{-5}$ ($\sim 4\,\sigma$), and $\chi^2_\nu(uvw1) = 2.18$ for 20 dof, nhp$= 1.6 \times 10^{-3}$ ($\sim 3\,\sigma$). The $uvw2$ magnitudes are mostly upper limits, and the 5 detections yield a mean of $uvw2 = 20.42 \pm 0.14$ mag. In Romano et al. (2009b) we reported a marginally significant (2–3 σ) increase of the u magnitude during the first recorded outburst of this source (2008-04-08, MJD 54565), while during the second outburst (2008-08-13, MJD 54692) the u magnitude is consistent with the mean for the whole campaign. The third reported outburst (2009-03-10, MJD 54901), like the second, shows no variation of the u magnitude, with respect to the mean of the campaign. Observations were also taken once in the v and b filters during 2009 as a follow-up ToO (obs. 00030987132), where we measure $v = 15.25 \pm 0.03$ and $b = 18.21 \pm 0.07$ mag. Both values are consistent with the ones obtained during and away from outbursts.

In Fig. 4 we show the UVOT $uvw1$ light curve of IGR J17544−2619. It is remarkably stable, as a fit against a constant yields $\chi^2_\nu(uvw1) = 1.08$ for 26 dof, nhp$= 0.35$. There are also a few observations performed in the other filters. We obtain $uvm2 = 20.3 \pm 0.3$ mag, $uvm2 = 20.0 \pm 0.3$ mag, $uvm2 = 19.9 \pm 0.2$ mag, $uvm2 = 19.9 \pm 0.3$ mag (obs. 00035056089, 00035056141, 00035056142, 00035056148, respectively), $uvw2 = 18.16 \pm 0.06$ mag and $uvw2 = 18.05 \pm 0.06$ mag (obs. 00035056143 and 00035056144), and $u = 15.25 \pm 0.09$ mag (obs. 00035056145). During the 2009 June 6 outburst (obs. 354221000, MJD 54988) all filters were used. The observed magnitudes are $u = 15.16 \pm 0.01$ mag, $b = 14.55 \pm 0.04$ mag, $uvw1 = 16.7 \pm 0.2$ mag. The $uvw1$ value is consistent with those obtained during the remainder of the campaign. The b magnitude is very close to the coincidence limit, therefore was heavily corrected for coincidence loss.

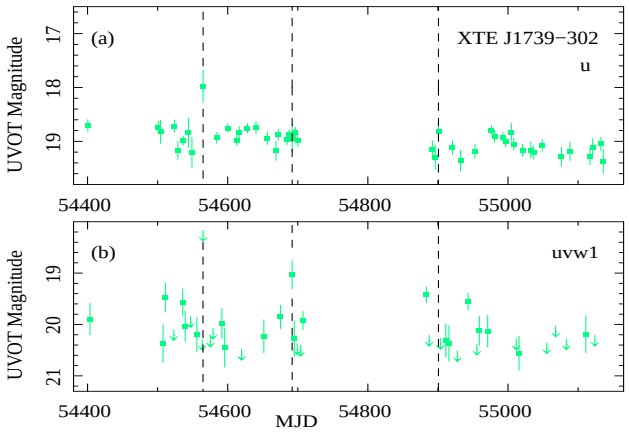


Figure 3. UVOT light curves of XTE J1739–302. The filters used are indicated in each panel. The vertical dashed lines mark the BAT outbursts.

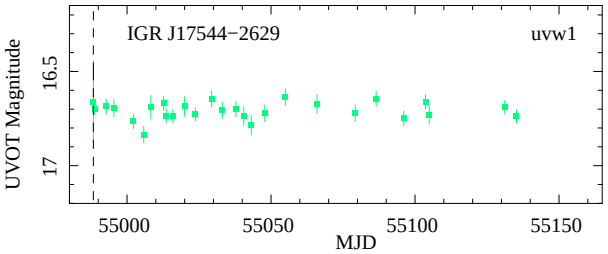


Figure 4. UVOT $uvw1$ light curve of IGR J17544−2619. The vertical dashed lines mark the BAT outbursts.

5 OUTBURSTS IN 2009

The year 2009 opened with the outburst of IGR J16479−4514 on January 29, which we reported on in Romano et al. (2009b). Here we analyze the data from three more outbursts caught from the sources in our sample.

5.1 IGR J17391−3021

XTE J1739−302 triggered the BAT on 2009 March 10 at 18:39:55 UT (image trigger=346069). We report the BAT light curve in the 15–25 keV band in Fig. 5. The time-averaged spectrum (T+0.0 to

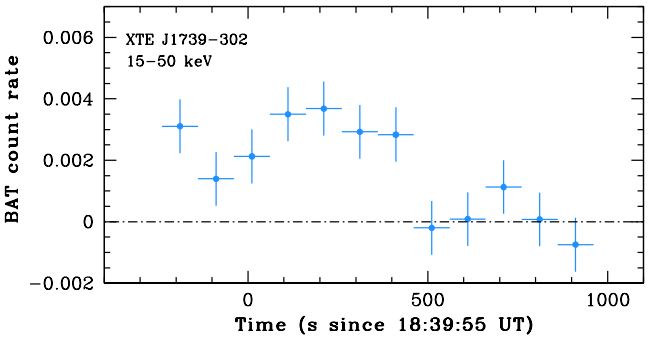


Figure 5. BAT light curve in the 15–50 keV band of the 2009 March 10 outburst of XTE J1739−302, in units of counts s^{-1} det^{-1}.

Table 7. Spectral fits of simultaneous XRT and BAT data of IGR J17544−2619 during the 2009 June 06 outburst.

Model	N_H[a]	Γ	E_c	E_f	Flux[c]	χ^2_ν/dof
POW[b]	$2.2^{+0.3}_{-0.2}$	$1.7^{+0.1}_{-0.1}$			2.6	1.53/117
HCT[b]	$1.0^{+0.2}_{-0.3}$	$0.6^{+0.2}_{-0.4}$	3^{+1}_{-1}	8^{+4}_{-3}	1.9	0.92/115
CPL[b]	$1.0^{+0.3}_{-0.2}$	$0.4^{+0.3}_{-0.3}$	7^{+4}_{-2}		1.9	0.94/116

[a] Absorbing column density is in units of 10^{22} cm^{-2}.

[b] POW=simple absorbed powerlaw. HCT= absorbed powerlaw with high energy cutoff E_c (keV), e-folding energy E_f (keV). CPL=cutoff powerlaw with energy cutoff E_c (keV).

[c] Unabsorbed 0.5–100 keV flux is in units of 10^{-9} erg cm^{-2} s^{-1}.

T+320.0 s) is best fit by a simple power-law model with a photon index of $2.8^{+0.8}_{-0.6}$, and the 15–50 keV flux is 7.6×10^{-10} erg cm^2 s^{-1}. *Swift* did not slew immediately in response to this trigger, so no NFI data were collected simultaneously with the BAT data. Observation 00030987107 (1.9 ks net exposure, see Table 2) was obtained as a high-priority ToO observation, instead. The light curve obtained between T+5257 s and T+10538 s since the trigger shows a mean count rate of 0.4–1 counts s^{-1}. The mean XRT/PC spectrum can be fit with an absorbed powerlaw with a photon index of $\Gamma = 1.1 \pm 0.4$ and an absorbing column density of $N_H = (3 \pm 1) \times 10^{22}$ cm^{-2} ($\chi^2_\nu = 1.1$ for 25 dof). The mean unabsorbed 2–10 keV flux is 9×10^{-11} erg cm^2 s^{-1}, which translates into a luminosity of 7×10^{34} erg s^{-1} (assuming a distance of 2.7 kpc, Rahoui et al. 2008). Further ToO observations were performed on 2009 March 11 (obs. 00030987108, 00030987109 in Table 2), when the XRT count rate was down to a few 10^{-2} counts s^{-1}. These spectral results are in general agreement with those obtained during previous outbursts, both in terms of hard photon index and in terms of a relatively lower column density (comparable with the out-of-outburst values).

5.2 IGR J17544−2619

Two outbursts of IGR J17544−2619 were caught during 2009. The first was observed by the BAT Transient Monitor as a sequence of bright flares. In the *Swift* pointings starting at 2009-03-15 23:52:40 UT (1024 s exposure) and at 2009-03-16 01:27:36 UT (1152 s) the source reached 0.026 ± 0.005 counts s^{-1} cm^{-2} (115 mCrab, 15–50 keV band) and 0.032 ± 0.005 counts s^{-1} cm^{-2} (140 mCrab), respectively. It then faded below detectability before re-brightening twice more on 2009 March 16: 95 mCrab in a 1152 s exposure beginning 06:16:40 UT and then to 85 mCrab in a 384 s exposure beginning at 09:25:52. XRT observations were performed as part of our regular monitoring on 2009 March 14 (see Table 3), ~ 46 h before the BAT outburst. A 3σ upper limit was obtained at 1.6×10^{-2} counts s^{-1}. A later observation, obtained as a ToO on 2009 March 16 (~ 16 h after the outburst), yielded a 3σ upper limit at 1.3×10^{-2} counts s^{-1}.

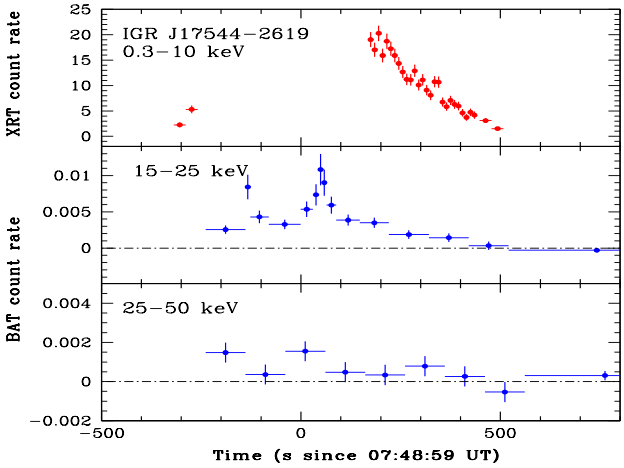


Figure 6. Light curves of the 2009 June 6 outburst of IGR J17544−2619. The XRT data preceding the outburst were collected as a pointed observation, part of our monitoring program. The BAT data are in units of counts s^{-1} det^{-1}.

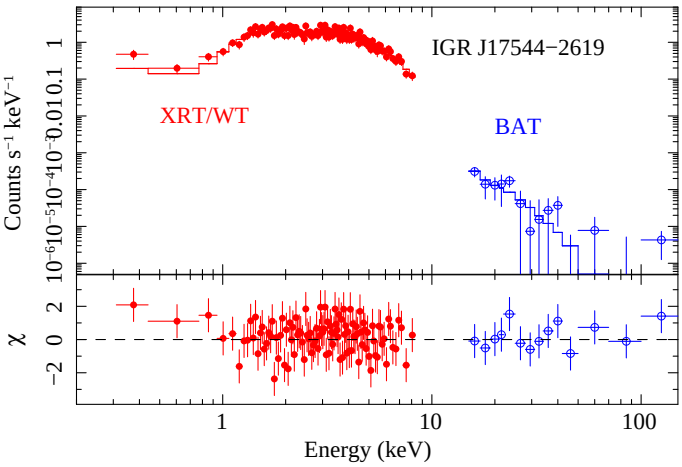


Figure 7. Spectroscopy of the 2009 June 6 outburst of IGR J17544−2619. **Top**: Data from the XRT/WT spectrum and simultaneous BAT spectrum fit with a CUTOFFPL model. **Bottom**: residuals in units of standard deviations.

IGR J17544−2619 triggered the BAT on 2009 June 06 at 07:48:59 UT (image trigger=354221). *Swift* immediately slewed to the target, so that the NFIs started observing about 164 s after the trigger. Figure 6 shows the XRT and BAT light curves, where it must be noted that the first two XRT points, preceding the out-

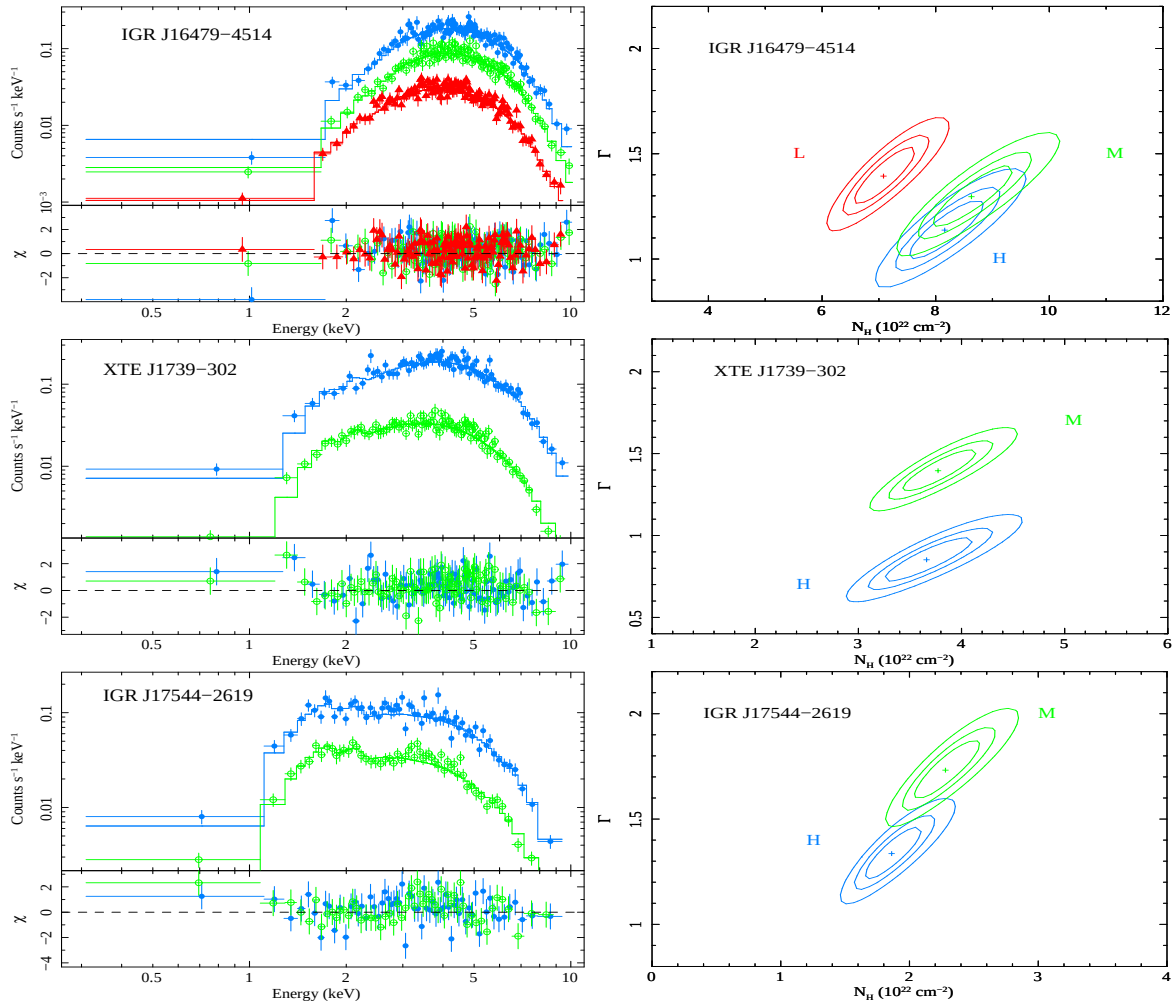


Figure 8. Spectroscopy of the 2007–2009 observing campaign. **Left.** Upper panels: XRT/PC data fit with an absorbed power law. Lower panels: the residuals of the fit (in units of standard deviations). Filled blue circles, green empty circles, and red filled triangles mark high, medium, and low states, respectively. **Right.** The $\Delta\chi^2 = 2.3$, 4.61 and 9.21 contour levels for the column density in units of 10^{22} cm^{-2} vs. the photon index, with best fits indicated by crosses. The labels L, M, and H mark low, medium, and high states, respectively.

burst, were collected as a pointed observation, part of our monitoring program. The initial XRT burst data (WT mode in observation 00354221000, see Table 3, 170–446 s since the trigger) show a decaying light curve with a count rate that started at about 20 counts s^{-1}. The following PC data (448–538s) seamlessly continue the decaying trend down to about 2 counts s^{-1}. The WT spectrum, extracted during the peak of the outburst (with a grade 0 selection to mitigate residual calibration uncertainties at low energies) results in a hard X–ray emission. When fit with an absorbed power law, we obtain a photon index of $1.05^{+0.15}_{-0.14}$ and a column density of $N_{\rm H} = (1.3 \pm 0.2) \times 10^{22}$ cm^{-2} ($\chi^2_\nu = 1.04$ for 104 dof). The unabsorbed 2–10 keV flux is 9.5×10^{-10} erg cm^{-2} s^{-1}. The PC spectrum (unabsorbed 2–10 keV flux $\sim 2 \times 10^{-10}$ erg cm^{-2} s^{-1}) fitted with a power-law model yields a photon index of 1.1 ± 0.7 and $N_{\rm H} = (1.2^{+1.2}_{-0.8}) \times 10^{22}$ cm^{-2} [Cash (1979) statistics and spectra binned to 1 count bin^{-1}; C–stat= 69.08 for 47 % of 10^4 Monte Carlo realizations with fit statistic less than C–stat], consistent with the WT data fit.

BAT mask-weighted spectra were extracted over time intervals strictly simultaneous with XRT data. We fit the simultaneous BAT+XRT spectra in the time interval 170–446 s since the BAT trigger, in the 0.3–10 keV and 15–150 keV energy bands for XRT and BAT, respectively. Factors were included in the fitting to allow for normalization uncertainties between the two instruments, constrained within their usual ranges (0.9–1.1). Table 7 reports our fits. A simple absorbed power-law model is clearly an inadequate representation of the broad band spectrum with a $\chi^2_\nu = 1.53$ for 117 dof). We then considered other curved models typically used to describe the X–ray emission from accreting pulsars in HMXBs, such as an absorbed power-law model with a high energy cut-off (HIGHECUT in XSPEC) and an absorbed power-law model with an exponential cutoff (CUTOFFPL). The latter models provide a satisfactory deconvolution of the 0.3–150 keV emission, resulting in

a hard powerlaw-like spectrum below 10 keV, with a roll over of the high energies when simultaneous XRT and BAT data fits are performed. Figure 7 shows the fits for the CUTOFFPL model.

6 OUT-OF-OUTBURST X–RAY SPECTROSCOPY

We characterize the spectral properties of the sources in several states, by accumulating the events in each observation when the source was not in outburst and a detection was achieved. We selected three count rate levels, CR_1, CR_2, and CR_3 (reported in Table 8) that would yield comparable statistics in the ranges $CR_1 < CR < CR_2$ (low), $CR_2 < CR < CR_3$ (medium), and $CR > CR_3$ (high). If the statistics did not allow this, then we only considered two intensity levels (high and medium). Exposure maps and ARF files were created following the procedure described in Romano et al. (2009b). The spectra were rebinned with a minimum of 20 counts per energy bin to allow χ^2 fitting. Each spectrum was fit in the energy range 0.3–10 keV with a single absorbed power law.

We accumulated all data for which no detections were obtained as single exposures (whose combined exposure is ΔT_Σ, reported in Table 5, column 2), and performed a detection. The resulting cumulative mean count rate for each object is reported in Table 5 (column 5). Spectra were also extracted from these event lists. They consisted of $\sim$ 200–300 counts each, so Cash statistics and spectra binned to 1 count bin^{-1} were used, instead. When fitting with free parameters, the best fit value for $N_{\rm H}$ turned out to be consistent with 0, i.e., well below the column derived from optical spectroscopy. We therefore performed fits by adopting as lower limit on the absorbing column the value derived from the Galactic extinction estimate along the line of sight to each source from Rahoui et al. (2008), with a conversion into Hydrogen column, $N_{\rm H} = 1.79 \times 10^{21} A_V$ cm^2 (Predehl & Schmitt 1995). Fig. 8 shows the spectra and contour plots of photon index vs. column density; the spectral parameters are reported in Table 8, where we also report the average 2–10 keV luminosities calculated by adopting distances of 4.9 kpc for IGR J16479−4514, 2.7 kpc for XTE J1739−302, and 3.6 kpc for IGR J17544−2619 determined by Rahoui et al. (2008) from optical spectroscopy of the supergiant companions. We also performed fits with an absorbed black body, obtaining consistent results with Romano et al. (2009b).

7 DISCUSSION

In this paper we report the results of a monitoring campaign with *Swift* that spans more than a two-year baseline. Thanks to the unique characteristics of *Swift* we can investigate the properties of SFTXs on several timescales (from minutes to days, to years) and in several intensity states (bright flares, intermediate intensity states, and down to almost quiescence).

During the second year of monitorning 2 different sources flared 3 times, and in 2 cases we obtained multi-wavelength observations (see Table 4). XTE J1739−302 triggered the BAT on 2009 March 10. Our results are in general agreement with those obtained during previous outbursts, both in terms of hard photon index and in terms of a relatively lower column density (comparable with the out-of outburst values). When IGR J17544−2619 triggered the BAT on 2009 June 06, simultaneous BAT and XRT data were collected, thus allowing broad band spectroscopy. The soft X–ray spectral properties observed during this flare are generally consistent with those observed with *Chandra* ($\Gamma = 0.73 \pm 0.13$, $N_{\rm H} = (1.36 \pm 0.22) \times 10^{22}$ cm^{-2}, peak flux of $\sim 3 \times 10^{-9}$ erg cm^{-2} s^{-1}; in't Zand 2005). However, when XRT and BAT data are jointly fit, an absorbed power-law model is inadequate in fitting the broad band spectrum, and more curvy models are required. We considered an absorbed power-law model with a high energy cut-off and an absorbed power-law model with an exponential cutoff, models typically used to describe the X–ray emission from accreting neutron stars in HMXBs. We obtained a good deconvolution of the 0.3–150 keV spectrum, characterized by a hard power law below 10 keV and a well-constrained cutoff at higher energies.

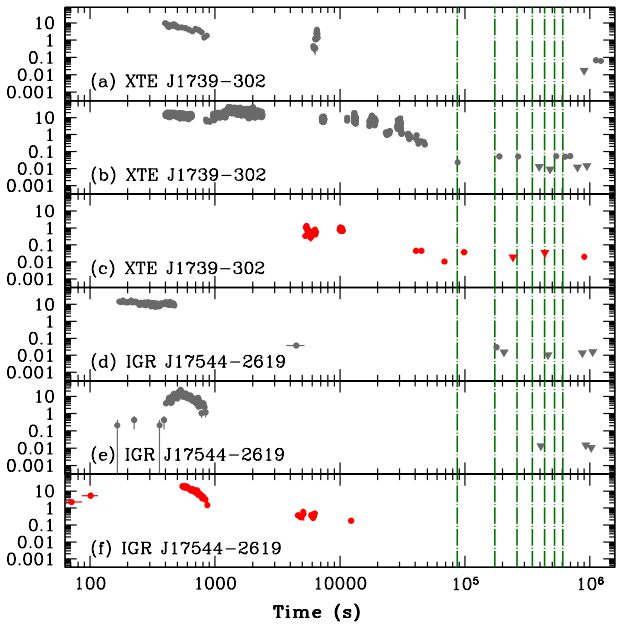


Figure 9. Light curves of the outbursts of SFXTs followed by *Swift*/XRT referred to their respective BAT triggers. Points denote detections, triangles 3σ upper limits. Red data points refer to observations presented here for the first time, while grey data points refer to data presented elsewhere. Note that where no data are plotted, no data were collected. Vertical dashed lines mark time intervals equal to 1 day, up to a week. Panels (a), (b) show the flares from XTE J1739−302 (2008-04-08, 2008-08-13; Sidoli et al. 2009c,a), while panel (c) refers to the 2009 March 10 flare reported here for the first time. Panels (d), (e) show the flares from IGR J17544–2916 (2008-03-31, 2008-09-04; Sidoli et al. 2009c,a), while panel (f) refers to the 2009 June 06 flare also reported here for the first time.

In Fig. 9 we compare the light curves of the most recent outbursts of XTE J1739−302 and IGR J17544−2619 (red points) observed by *Swift* during the second year of monitoring, together with the previous outbursts of these sources followed by *Swift*/XRT (grey points). The light curves are referred to their respective BAT triggers (unless the flare did not trigger the BAT, Fig. 9e). The most complete and deep set of X–ray observations of an outburst of a SFXT is the one of the periodic SFXT IGR J11215−5952 (Romano et al. 2007; Sidoli et al. 2007; Romano et al. 2009c), which was instrumental in discovering that the accretion phase during the bright outbursts lasts much longer than a few hours, as seen by lower-sensitivity instruments, and contrary to what initially thought at the time of the

Table 8. XRT spectroscopy of the three SFXTs (2007–2009 data set).

Name Absorbed power law	Spectrum	Rate (counts s^{-1})	$N_{\rm H}$ (10^{22} cm^{-2})	Parameter Γ	Flux[a] (2–10 keV)	Luminosity[b] (2–10 keV)	χ^2_ν/dof[c] Cstat(%)
IGR J16479−4514	high	>0.55	$8.2^{+0.8}_{-0.7}$	$1.1^{+0.2}_{-0.2}$	120	5	1.2/193
	medium	[0.22–0.55[	$8.6^{+0.8}_{-0.8}$	$1.3^{+0.2}_{-0.2}$	53	2	0.9/197
	low	[0.06–0.22[	$7.1^{+0.6}_{-0.6}$	$1.4^{+0.2}_{-0.1}$	17	0.7	1.0/205
	very low[d]	<0.06	$3.3^{+0.4}_{-0.0}$	$1.8^{+0.3}_{-0.2}$	1.3	0.04	302.5(99.5)
XTE J1739−302	high	>0.405	$3.7^{+0.5}_{-0.4}$	$0.8^{+0.2}_{-0.1}$	120	1	1.0/160
	medium	[0.07–0.405[	$3.8^{+0.4}_{-0.4}$	$1.4^{+0.1}_{-0.1}$	18	0.2	0.9/164
	very low[d]	<0.07	$1.7^{+0.1}_{-0.0}$	$1.4^{+0.2}_{-0.2}$	0.5	0.004	321.9(98.6)
IGR J17544−2619	high	>0.25	$1.9^{+0.3}_{-0.2}$	$1.3^{+0.1}_{-0.1}$	46	0.8	1.0/118
	medium	[0.07–0.25[	$2.3^{+0.3}_{-0.3}$	$1.7^{+0.2}_{-0.2}$	14	0.3	1.0/108
	very low[d]	<0.07	$1.1^{+0.1}_{-0.0}$	$2.1^{+0.2}_{-0.2}$	0.2	0.003	183.1(85.1)

[a] Average observed 2–10 keV fluxes in units of 10^{-12} erg cm^{-2} s^{-1}.

[b] Average 2–10 keV X–ray luminosities in units of 10^{35} erg s^{-1} calculated adopting distances determined by Rahoui et al. (2008).

[c] Reduced χ^2 and dof, or Cash statistics C–stat and percentage of realizations (10^4 trials) with statistic > Cstat.

[d] Fit performed with constrained column density (see Sect 6).

discovery of this new class of sources (e.g., Sguera et al. 2005). This behaviour is now found to be a common characteristic of the whole sample of SFXTs followed by *Swift*, as our observations on IGR J16479−4514, IGR J08408−4503, and SAX J1818.6−1703 demonstrate (Romano et al. 2009b,a; Sidoli et al. 2009b, respectively; the vertical dashed lines in Fig. 9 mark time intervals equal to 1 day, up to a week). In the same manner, our observations show that both the large dynamical range (up to 4 orders of magnitude) in flux and a multiple-peaked structure of the light curves of the bright outbursts are equally common characteristics of the sample.

In the optical/UV we see only marginal variability in the u and $uvw1$ magnitudes of XTE J1739−302, and we could exclude a variation of flux corresponding to the X–ray outburst. The $uvw1$ light curve of IGR J17544−2619 is observed to be remarkably stable. This is consistent with the optical/UV emission being dominated by the constant contribution of the companion stars.

Variability in the X–ray flux is observed at all timescales and intensity ranges we can probe. Figure 10 shows, for each of the monitored sources, a montage of time sequences of the *Swift*/XRT data where detection was achieved (binned at a 100 s and 20 s resolution for PC and WT data, respectively) and with observing and orbital gaps removed from the time axis. Superimposed on the day-to-day variability (best shown in Fig. 1 which is binned to a day resolution) is intra-day flaring. As Fig. 10 shows, the latter involves flux variations up to one order of magnitude that can occur down to timescales as short as an XRT snapshot ($\lesssim$ 1 ks). This remarkable short time scale variability cannot be accounted for by accretion from a homogeneous wind. On the contrary, it can be naturally explained by the accretion of single clumps composing the donor wind, independently on the detailed geometrical and kinematical properties of the wind and the properties of the accreting compact object. If, for example, we assume that each of these short flares is caused by the accretion of a single clump onto the NS (e.g., in't Zand 2005), then its mass can be estimated (Walter & Zurita Heras 2007) as $M_{\rm cl} = 7.5 \times 10^{21}\ (L_{\rm X,36})(t_{\rm fl,3ks})^3$ g, where $L_{\rm X,36}$ is the average X-ray luminosity in units of 10^{36} erg s^{-1}, $t_{\rm fl,3ks}$ is the duration of the flares in units of 3 ks. We can confidently identify flares down to a count rate in the order of 0.1 counts s^{-1} (within a snapshot of about 1 ks; see Fig. 10); these correspond to luminosities in the order of 2–6 $\times$ 10^{34} erg s^{-1}, which yield $M_{\rm cl} \sim 0.3$–2×10^{19} g. These masses are about those expected (Walter & Zurita Heras 2007) to be responsible of short flares, below the *INTEGRAL* detection threshold and which, if frequent enough, may significantly contribute to the mass-loss rate.

Our *Swift* monitoring campaign has demonstrated for the first time that X–ray emission from SFXTs is present outside the bright outbursts (Sidoli et al. 2008b; Romano et al. 2009b), although at a much lower level thus showing how frequent and typical in SFXTs is accretion at a low level rate. In this paper we refined the intensity selected spectroscopy of the out-of-outburst emission, by adopting absorbed power laws which yield hard power law photon indices ($\Gamma\sim$1–2). All these results are consistent with our findings in Romano et al. (2009b) and show that accretion occurs over several orders of magnitude in luminosity (3 for XTE J1739−302 and 2 for the others; Table 8), even when excluding the bright outbursts. In particular, the lowest luminosities we could study with *Swift* are 4×10^{32} erg s^{-1} and 3×10^{32} erg s^{-1} (2–10 keV; 'very low' intensity level in Table 8) for XTE J1739–302 and IGR J17544−2619, respectively. These low luminosities are not consistent with Bondi-Hoyle accretion from a spherically symmetric steady wind (Bondi & Hoyle 1944), as previously reported by Drave et al. (2010) and Clark et al. (2009) for these two SFXTs, thus arguing for a clumpy nature of the accreting wind. This is consistent with our findings on short timescale variability, which also requires inhomogeneities in the wind.

In the following, we assess the percentage of time each source spends at a given flux state. Figure 11 shows the distributions of the observed count rates after removal of the observations where a detection was not achieved (same sample as in Fig. 10, with PC and WT data binned at 100 s). In all cases a roughly Gaussian shape is observed, with a broad peak at $\approx$ 0.1 counts s^{-1}, and a clear cut at the detection limit for 100 s at the low end. In particular, when the distributions are fit with a Gaussian function we find that their means and σ are 0.12 and 3.4 counts s^{-1} for IGR J16479−4514, 0.06 and 4.9 counts s^{-1} for XTE J1739–302, and 0.13 and 3.1

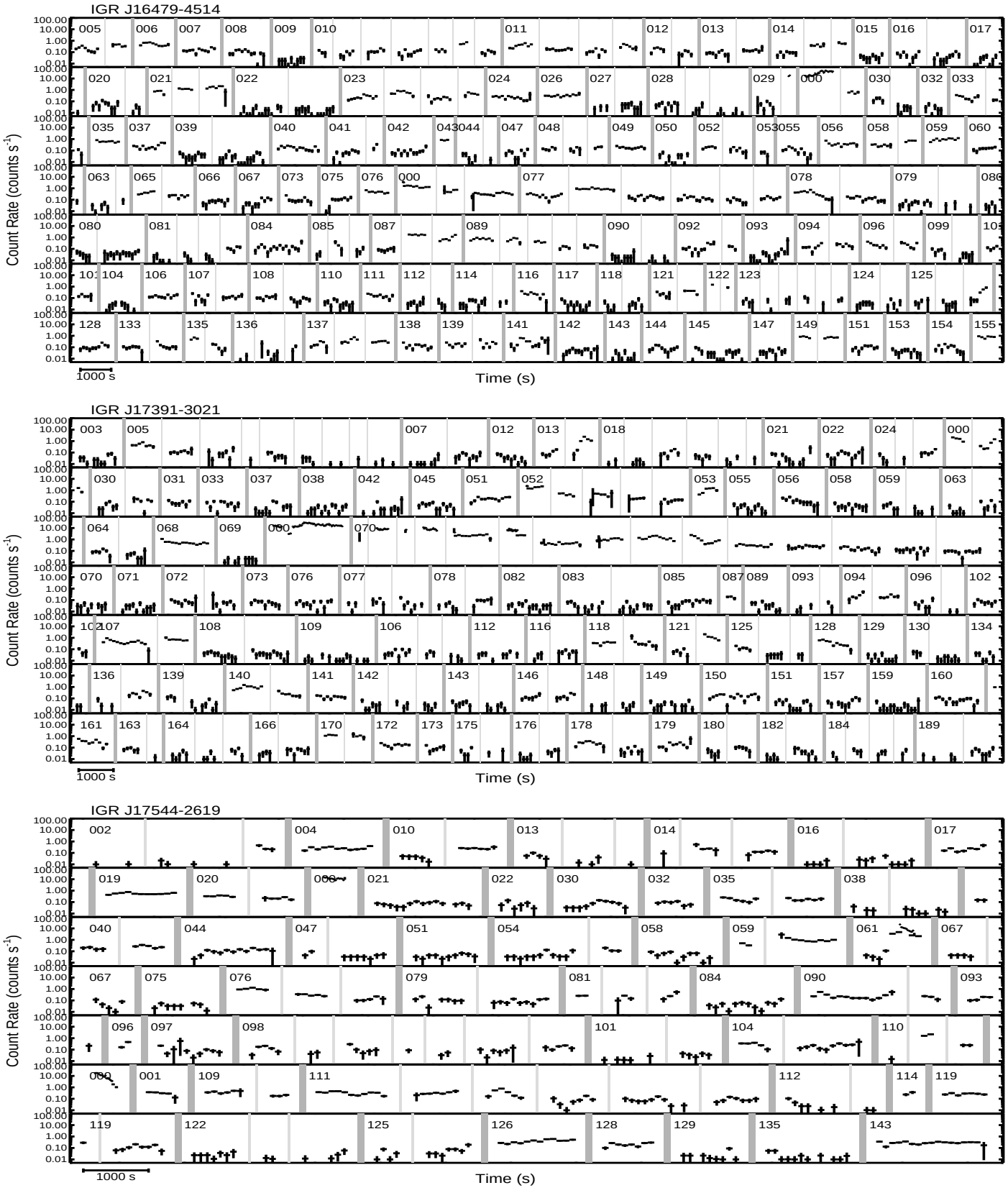


Figure 10. *Swift*/XRT (0.2–10 keV) montage of time sequences. The numbers in the plot identify each observing sequence (see Table 1, 2, and 3), with 000 marking outburts. Non observing intervals and orbital gaps have been cut out from the time axis and replaced by thick vertical bars to separate different sequences and thin grey bars to separate different orbits within each sequence. Each point represents a 100 s bin in PC and a 20 s bin in WT modes. As a reference, on the bottom-left we show the 1000 s time unit. The light curves are corrected for pile-up PSF losses, vignetting and background-subtracted.

counts s^{-1} for IGR J17544−2619, respectively. This indicates that the most probable flux level at which a random observation will find these sources, when detected, is 3×10^{-11}, 9×10^{-12}, and 1×10^{-11} erg cm^{-2} s^{-1} (unabsorbed 2–10 keV, obtained using the medium spectra in Table 8), corresponding to luminosities of $\sim 8 \times 10^{34}$, 8×10^{33}, and 2×10^{34} erg s^{-1}, respectively. Figure 11 also shows the hint of an excess at $\gtrsim 10$ counts s^{-1}. Since this count rate is where the WT data of the outbursts are concentrated, we also show them in the insets (dashed histograms) binned at 20 s resolution, which is more appropriate for such count rates. In this case, a clear peak emerges to represent the flaring state of the sources.

We have also calculated the time each source spends *undetected* down to a flux limit of 1–3$\times 10^{-12}$ erg cm^{-2} s^{-1}, and we obtain IDC $= 19, 39, 55$ %, for IGR J16479−4514, XTE J1739–302, and IGR J17544−2619, respectively, with an estimated error of ~ 5 %. We note that these values are based on the whole 2-year campaign, and that the IDC calculated with the observations of 2009 only is $21, 39, 55$ %. These results can be compared with the ones reported in Romano et al. (2009b), where we obtained IDC $= 17, 39, 55$ %, for IGR J16479−4514, XTE J1739–302, and IGR J17544−2619, respectively. We now have a baseline twice as long and almost a factor of two higher exposure; the sampling of the light curves has slightly changed during 2009. Nevertheless, the calculated IDC values are remarkably stable, which is indicative of the robustness of this method with respect to the sampling pace. Considering our monitoring as a casual sampling of the light curve for two years, we can also infer that the time these sources spend in bright outbursts is between 3 and 5 % of the total.

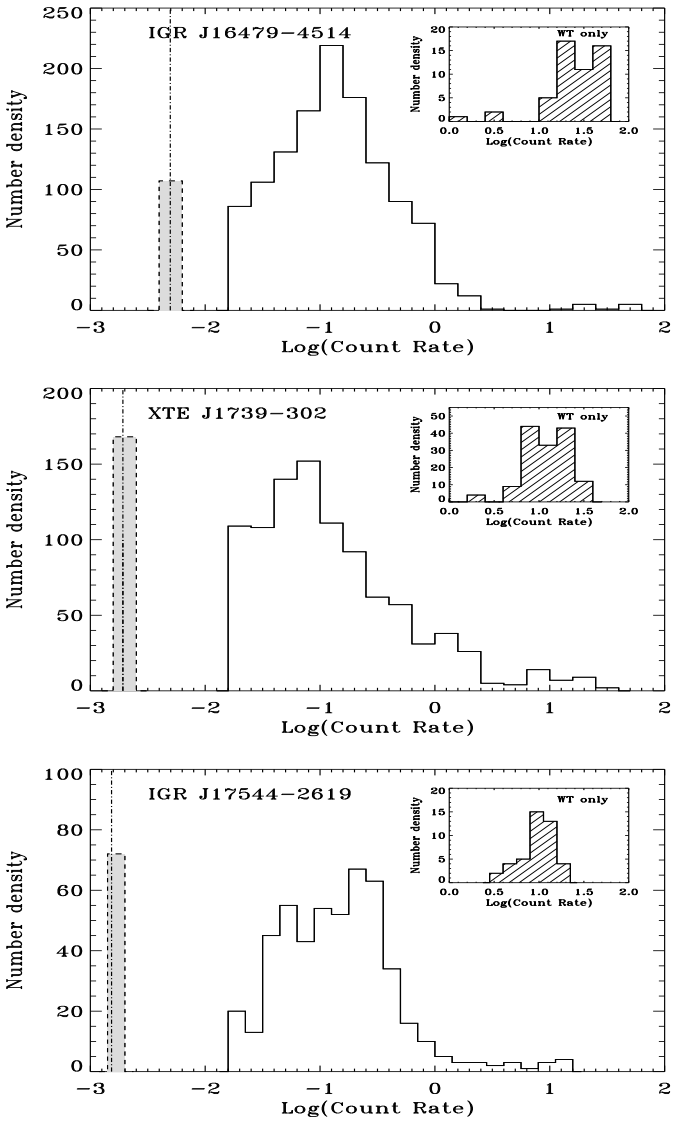


Figure 11. Distribution of the count rates when the XRT light curves are binned at 100 s. The vertical lines correspond to the background. The hashed histograms are points which are consistent with a zero count rate. The insets show the subset of WT data only, when binned at 20 s.

ACKNOWLEDGMENTS

PR dedicates this effort to her grandmother, G. Ghedin; she could not follow her aspiration, yet worked hard so that others could. We acknowledge the input from our colleagues along the way during this large project, in particular A. Beardmore, M.M. Chester, L. Ducci, C. Guidorzi, T. Mineo, M. Perri. We thank the *Swift* team duty scientists and science planners. We also thank the remainder of the *Swift* XRT, BAT, and UVOT teams, S. Barthelmy and J.A. Nousek in particular, for their invaluable help and support with the planning and execution of the observing strategy. We also thank the anonymous referee for comments that helped improve the paper. This work was supported at PSU by NASA contract NAS5-00136. HAK was supported by the *Swift* project.

REFERENCES

Barthelmy S. D., Barbier L. M., Cummings J. R., et al. 2005, Space Science Reviews, 120, 143
Blay P., Martínez-Núñez S., Negueruela I., et al. 2008, A&A, 489, 669
Bondi H., Hoyle F., 1944, MNRAS, 104, 273
Bozzo E., Falanga M., Stella L., 2008, ApJ, 683, 1031
Bozzo E., Giunta A., Stella L., Falanga M., Israel G., Campana S., 2009, A&A, 502, 21
Bozzo E., Stella L., Israel G., Falanga M., Campana S., 2008, MNRAS, 391, L108
Burrows D. N., Hill J. E., Nousek J. A., et al. 2005, Space Science Reviews, 120, 165
Cash W., 1979, ApJ, 228, 939
Clark D. J., Hill A. B., Bird A. J., McBride V. A., Scaringi S., Dean A. J., 2009, MNRAS, 399, L113
Drave S. P., Clark D. J., Bird A. J., McBride V. A., Hill A. B., Sguera V., Scaringi S., Bazzano A., 2010, MNRAS, in press, arXiv:1007.3379
Grebenev S. A., Lutovinov A. A., Sunyaev R. A., 2003, Astron. Tel., 192
Grebenev S. A., Rodriguez J., Westergaard N. J., Sunyaev R. A., Oosterbroek T., 2004, Astron. Tel., 252
in't Zand J., Heise J., Ubertini P., Bazzano A., Markwardt C., 2004, in V. Schoenfelder, G. Lichti, & C. Winkler ed., 5th INTEGRAL Workshop on the INTEGRAL Universe Vol. 552 of ESA Special Publication, A BeppoSAX-WFC Viewpoint of New INTEGRAL Sources, Particularly IGR J17544-2619, pp 427
in't Zand J. J. M., 2005, A&A, 441, L1

Jain C., Paul B., Dutta A., 2009, MNRAS, 397, L11
Kennea J. A., Pagani C., Markwardt C., Blustin A., Cummings J., Nousek J., Gehrels N., 2005, Astron. Tel., 599
Krimm H., Barbier L., Barthelmy S. D., et al. 2006, Astron. Tel., 904
Krimm H. A., Barthelmy S. D., Barbier L., et al. 2007, Astron. Tel., 1265
Krimm H. A., Barthelmy S. D., Cummings J. R., Markwardt C. B., Skinner G., Tueller J., Swift/BAT Team 2008, in AAS/High Energy Astrophysics Division Vol. 10 of AAS/High Energy Astrophysics Division, Status of the Swift/BAT Hard X-ray Transient Monitor. p. #07.01
Krimm H. A., Romano P., Sidoli L., 2009, Astron. Tel., 1971
Kuulkers E., Oneca D. R., Brandt S., et al. 2007, Astron. Tel., 1266
La Parola V., Romano P., Sidoli L., et al. 2009, Astron. Tel., 1929
Markwardt C. B., Krimm H. A., 2006, Astron. Tel., 816
Molkov S., Mowlavi N., Goldwurm A., Strong A., Lund N., Paul J., Oosterbroek T., 2003, Astron. Tel., 176
Negueruela I., Smith D. M., Harrison T. E., Torrejón J. M., 2006, ApJ, 638, 982
Negueruela I., Torrejón J. M., Reig P., Ribó M., Smith D. M., 2008, 1010, 252
Pellizza L. J., Chaty S., Negueruela I., 2006, A&A, 455, 653
Poole T. S., Breeveld A. A., Page M. J., et al. 2008, MNRAS, 383, 627
Predehl P., Schmitt J. H. M. M., 1995, A&A, 293, 889
Rahoui F., Chaty S., Lagage P.-O., Pantin E., 2008, A&A, 484, 801
Rampy R. A., Smith D. M., Negueruela I., 2009, ApJ, 707, 243
Romano P., Cusumano G., Sidoli L., et al. 2008a, Astron. Tel., 1697
Romano P., Guidorzi C., Sidoli L., et al. 2008b, Astron. Tel., 1659
Romano P., Sidoli L., Cusumano G., et al. 2009a, MNRAS, 392, 45
Romano P., Sidoli L., Cusumano G., et al. 2009b, MNRAS, 399, 2021
Romano P., Sidoli L., Cusumano G., Vercellone S., Mangano V., Krimm H. A., 2009c, ApJ, 696, 2068
Romano P., Sidoli L., Krimm H. A., et al. 2009d, Astron. Tel., 1961
Romano P., Sidoli L., Mangano V., et al. 2009e, Astron. Tel., 1920
Romano P., Sidoli L., Mangano V., et al. 2008c, Astron. Tel., 1466
Romano P., Sidoli L., Mangano V., Mereghetti S., Cusumano G., 2007, A&A, 469, L5
Romano P., Sidoli L., Mangano V., et al. 2008d, ApJL, 680, L137
Romano P., Sidoli L., Vercellone S., et al. 2009f, Astron. Tel., 2069
Roming P. W. A., Kennedy T. E., Mason K. O., et al. 2005, Space Science Reviews, 120, 95
Sguera V., Barlow E. J., Bird A. J., et al. 2005, A&A, 444, 221
Sguera V., Bazzano A., Bird A. J., et al. 2006, ApJ, 646, 452
Sidoli L., Paizis A., Mereghetti S., 2006, A&A, 450, L9
Sidoli L., Romano P., Ducci L., et al. 2009a, MNRAS, 397, 1528
Sidoli L., Romano P., Esposito P., et al. 2009b, MNRAS, 400, 258
Sidoli L., Romano P., Mangano V., et al. 2009c, ApJ, 690, 120
Sidoli L., Romano P., Mangano V., et al. 2008a, Astron. Tel., 1454
Sidoli L., Romano P., Mangano V., et al. 2008b, ApJ, 687, 1230
Sidoli L., Romano P., Mereghetti S., Paizis A., Vercellone S., Mangano V., Götz D., 2007, A&A, 476, 1307
Smith D. M., Main D., Marshall F., Swank J., Heindl W. A., Leventhal M., in 't Zand J. J. M., Heise J., 1998, ApJL, 501, L181
Sunyaev R. A., Grebenev S. A., Lutovinov A. A., Rodriguez J., Mereghetti S., Gotz D., Courvoisier T., 2003, Astron. Tel., 190
Vaughan S., Goad M. R., Beardmore A. P., et al. 2006, ApJ, 638, 920
Walter R., Zurita Heras J., 2007, A&A, 476, 335
Walter R., Zurita Heras J., Bassani L., et al. 2006, A&A, 453, 133

This paper has been typeset from a TEX/ LATEX file prepared by the author.

Table 1. Observation log for IGR J16479−4514.

Sequence	Instrument/Mode	Start time (UT) (yyyy-mm-dd hh:mm:ss)	End time (UT) (yyyy-mm-dd hh:mm:ss)	Net Exposure (s)
00030296096	PC	2009-02-19 21:23:39	2009-02-19 23:11:56	1178
00030296097	PC	2009-02-23 15:15:37	2009-02-23 17:08:58	1925
00030296098	PC	2009-02-26 20:38:22	2009-02-26 22:21:58	902
00030296099	PC	2009-03-01 01:36:58	2009-03-01 03:20:57	1014
00030296101	PC	2009-03-08 01:58:11	2009-03-08 02:11:58	813
00030296102	PC	2009-03-12 12:00:26	2009-03-12 12:13:56	794
00030296103	PC	2009-03-15 17:26:03	2009-03-15 17:42:56	996
00030296104	PC	2009-03-19 22:41:22	2009-03-19 22:57:50	987
00030296105	PC	2009-03-23 05:11:51	2009-03-23 05:34:57	1348
00030296106	PC	2009-03-26 23:17:55	2009-03-26 23:33:56	949
00030296107	PC	2009-03-29 20:20:10	2009-03-29 22:05:55	1152
00030296108	PC	2009-04-02 10:51:38	2009-04-02 12:44:57	1209
00030296110	PC	2009-04-09 22:57:46	2009-04-09 23:13:56	962
00030296111	PC	2009-04-12 00:46:56	2009-04-12 01:01:54	850
00030296112	PC	2009-04-16 01:03:12	2009-04-16 02:49:58	871
00030296114	PC	2009-04-23 06:35:10	2009-04-23 08:25:57	1128
00030296116	PC	2009-05-03 20:31:05	2009-05-03 20:44:58	824
00030296117	PC	2009-05-07 07:45:46	2009-05-07 08:02:56	1021
00030296118	PC	2009-05-14 21:31:15	2009-05-14 23:13:56	771
00030296119	PC	2009-05-17 18:25:09	2009-05-17 18:26:57	108
00030296120	PC	2009-05-21 02:33:56	2009-05-21 04:15:57	817
00030296121	PC	2009-05-28 16:01:59	2009-05-28 17:44:57	831
00030296122	PC	2009-06-04 09:00:40	2009-06-04 10:22:56	66
00030296123	PC	2009-06-10 14:19:27	2009-06-10 22:31:57	1087
00030296124	PC	2009-06-11 09:17:46	2009-06-11 11:03:57	1166
00030296125	PC	2009-06-14 12:57:00	2009-06-14 16:25:57	1344
00030296127	PC	2009-06-22 21:41:15	2009-06-22 23:24:57	895
00030296128	PC	2009-06-25 15:35:42	2009-06-25 15:51:58	960
00030296129	PC	2009-06-29 02:03:38	2009-06-29 16:34:57	412
00030296130	PC	2009-07-02 22:56:56	2009-07-02 23:15:57	1117
00030296131	PC	2009-07-06 23:03:27	2009-07-06 23:41:57	929
00030296132	PC	2009-07-09 20:41:44	2009-07-09 23:55:57	393
00030296133	PC	2009-07-12 07:45:29	2009-07-12 09:29:58	1199
00030296134	PC	2009-07-19 18:04:32	2009-07-19 18:13:56	564
00030296135	PC	2009-07-23 15:17:39	2009-07-23 17:03:56	695
00030296136	PC	2009-07-26 13:36:28	2009-07-26 17:00:57	974
00030296137	PC	2009-07-30 01:03:16	2009-07-30 04:24:56	1608
00030296138	PC	2009-08-02 19:20:12	2009-08-02 19:36:57	982
00030296139	PC	2009-08-06 12:58:49	2009-08-06 14:46:57	1177
00030296141	PC	2009-08-13 02:28:41	2009-08-13 02:48:45	817
00030296142	PC	2009-08-20 17:46:23	2009-08-20 18:04:57	1111
00030296143	PC	2009-08-23 11:50:59	2009-08-23 12:07:57	1004
00030296144	PC	2009-08-27 05:46:01	2009-08-27 06:02:57	994
00030296145	PC	2009-08-30 05:52:17	2009-08-30 06:20:57	1710
00030296146	PC	2009-09-10 15:02:38	2009-09-10 15:18:58	967
00030296147	PC	2009-09-13 15:20:34	2009-09-13 15:36:57	975
00030296148	PC	2009-09-17 02:48:04	2009-09-17 03:05:57	1056
00030296149	PC	2009-09-20 06:00:19	2009-09-20 07:42:56	785
00030296150	PC	2009-09-27 14:53:56	2009-09-27 16:41:57	1127
00030296151	PC	2009-10-01 21:50:58	2009-10-01 22:05:58	884
00030296152	PC	2009-10-04 02:43:42	2009-10-04 02:59:57	943
00030296153	PC	2009-10-08 03:12:19	2009-10-08 03:28:57	984
00030296154	PC	2009-10-18 13:39:21	2009-10-18 13:54:56	905
00030296155	PC	2009-10-25 08:04:27	2009-10-25 08:13:56	569

Table 2. Observation log for IGR J17391−3021.

Sequence	Instrument/Mode	Start time (UT) (yyyy-mm-dd hh:mm:ss)	End time (UT) (yyyy-mm-dd hh:mm:ss)	Net Exposure (s)
00030987098	PC	2009-02-21 13:32:13	2009-02-21 15:19:57	1382
00030987099	PC	2009-02-23 07:26:20	2009-02-23 09:11:58	1354
00030987100	PC	2009-02-25 14:13:53	2009-02-25 15:56:58	1123
00030987101	PC	2009-02-27 23:51:23	2009-02-27 23:59:44	487
00030987102	PC	2009-03-02 01:42:07	2009-03-02 01:57:57	939
00030987103	PC	2009-03-04 00:28:00	2009-03-04 03:43:57	811
00030987104	PC	2009-03-06 02:12:57	2009-03-06 05:35:56	833
00030987105	PC	2009-03-08 03:33:33	2009-03-08 03:53:56	1201
00346069000	BAT/evt	2009-03-10 18:36:00	2009-03-10 18:56:02	1202
00030987107	PC	2009-03-10 20:07:35	2009-03-10 21:35:54	1883
00030987108	PC	2009-03-11 05:52:47	2009-03-11 07:19:57	1975
00030987109	PC	2009-03-11 13:28:45	2009-03-11 14:01:56	1976
00030987106	PC	2009-03-11 20:16:24	2009-03-11 23:44:55	1361
00030987110	PC	2009-03-13 13:55:19	2009-03-13 14:11:57	986
00030987111	PC	2009-03-15 19:04:51	2009-03-15 20:45:57	862
00030987112	PC	2009-03-21 05:03:14	2009-03-21 05:24:56	1288
00030987113	PC	2009-03-23 22:53:06	2009-03-23 23:14:58	1257
00030987114	PC	2009-03-25 16:54:16	2009-03-25 18:43:56	1322
00030987115	PC	2009-03-27 17:10:56	2009-03-27 17:15:57	282
00030987116	PC	2009-03-30 17:19:23	2009-03-30 18:59:56	900
00030987117	PC	2009-04-01 14:14:04	2009-04-01 15:58:58	180
00030987118	PC	2009-04-06 16:19:14	2009-04-06 18:06:56	1353
00030987120	PC	2009-04-11 07:15:28	2009-04-11 08:59:56	869
00030987121	PC	2009-04-12 05:47:30	2009-04-12 07:31:29	801
00030987122	PC	2009-04-17 14:04:05	2009-04-17 14:23:56	1186
00030987124	PC	2009-04-22 01:44:10	2009-04-22 03:27:57	1155
00030987125	PC	2009-04-24 01:58:43	2009-04-24 04:59:57	1189
00030987126	PC	2009-04-29 17:03:39	2009-04-29 20:20:56	1162
00030987127	PC	2009-05-01 20:17:41	2009-05-01 20:33:56	961
00030987128	PC	2009-05-04 12:15:55	2009-05-04 12:31:55	943
00030987129	PC	2009-05-06 23:45:39	2009-05-06 23:59:57	856
00030987130	PC	2009-05-08 00:03:19	2009-05-08 05:09:56	919
00030987131	PC	2009-05-15 17:00:32	2009-05-15 18:43:56	927
00030987132	PC	2009-05-18 15:18:35	2009-05-18 15:32:57	845
00030987133	PC	2009-05-20 01:18:12	2009-05-20 01:33:57	933
00030987134	PC	2009-05-22 23:55:04	2009-05-23 00:07:56	753
00030987135	PC	2009-05-25 09:40:45	2009-05-25 11:27:56	1102
00030987136	PC	2009-05-27 06:23:01	2009-05-27 09:43:56	1295
00030987137	PC	2009-05-29 21:36:23	2009-05-29 23:15:56	812
00030987139	PC	2009-06-03 04:22:19	2009-06-03 05:34:57	957
00030987140	PC	2009-06-10 14:26:00	2009-06-10 16:16:57	1484
00030987141	PC	2009-06-12 04:41:14	2009-06-12 04:55:57	875
00030987142	PC	2009-06-14 13:04:58	2009-06-14 16:33:57	1465
00030987143	PC	2009-06-17 11:59:25	2009-06-17 13:45:57	1253
00030987144	PC	2009-06-19 13:34:34	2009-06-19 15:19:58	1106
00030987145	PC	2009-06-22 21:50:01	2009-06-22 21:55:05	289
00030987146	PC	2009-06-24 20:34:06	2009-06-24 22:18:58	1009
00030987147	PC	2009-06-26 04:38:26	2009-06-26 08:12:08	919
00030987148	PC	2009-06-29 18:07:36	2009-06-29 19:50:58	837
00030987149	PC	2009-07-01 13:15:25	2009-07-01 13:36:56	1288
00030987150	PC	2009-07-03 17:58:50	2009-07-03 18:22:57	1439
00030987151	PC	2009-07-08 18:46:26	2009-07-08 19:04:57	1086
00030987152	PC	2009-07-10 17:34:35	2009-07-10 20:32:56	777
00030987154	PC	2009-07-17 09:58:00	2009-07-17 11:34:58	1049
00030987155	PC	2009-07-20 13:27:01	2009-07-20 15:09:56	535
00030987156	PC	2009-07-22 18:22:50	2009-07-22 18:39:56	1019
00030987157	PC	2009-07-24 15:24:43	2009-07-24 15:40:56	966
00030987159	PC	2009-07-29 10:44:26	2009-07-29 11:04:57	1218
00030987160	PC	2009-08-03 21:05:26	2009-08-03 21:26:57	1273
00030987161	PC	2009-08-05 21:10:28	2009-08-05 21:26:56	978
00030987162	PC	2009-08-07 08:19:05	2009-08-07 10:08:56	1262
00030987163	PC	2009-08-10 21:30:24	2009-08-10 23:14:57	881

Table 2. Observation log for IGR J17391−3021. Continued.

Sequence	Instrument/Mode	Start time (UT) (yyyy-mm-dd hh:mm:ss)	End time (UT) (yyyy-mm-dd hh:mm:ss)	Net Exposure (s)
00030987164	PC	2009-08-12 05:38:33	2009-08-12 08:57:57	1198
00030987166	PC	2009-08-22 14:39:23	2009-08-22 16:56:56	900
00030987167	PC	2009-08-24 21:17:04	2009-08-24 21:27:56	648
00030987168	PC	2009-08-26 02:13:22	2009-08-26 02:31:58	1080
00030987169	PC	2009-08-31 04:16:51	2009-08-31 04:42:56	1555
00030987170	PC	2009-09-02 06:33:58	2009-09-02 08:15:57	570
00030987171	PC	2009-09-09 06:40:15	2009-09-09 08:23:56	1045
00030987172	PC	2009-09-11 08:46:47	2009-09-11 09:01:57	904
00030987173	PC	2009-09-14 12:22:51	2009-09-14 12:31:57	528
00030987174	PC	2009-09-16 15:36:36	2009-09-16 15:52:57	968
00030987175	PC	2009-09-18 10:47:06	2009-09-18 12:35:57	834
00030987176	PC	2009-09-21 02:55:51	2009-09-21 04:39:56	808
00030987177	PC	2009-09-23 00:03:21	2009-09-23 12:59:58	844
00030987178	PC	2009-09-28 21:39:16	2009-09-28 23:24:56	1383
00030987179	PC	2009-10-02 21:47:31	2009-10-02 22:02:57	904
00030987180	PC	2009-10-05 20:35:06	2009-10-05 22:19:57	1052
00030987181	PC	2009-10-07 01:26:48	2009-10-07 03:11:56	1031
00030987182	PC	2009-10-09 01:50:41	2009-10-09 03:33:55	1287
00030987183	PC	2009-10-12 21:12:04	2009-10-12 22:55:58	1426
00030987184	PC	2009-10-14 16:28:06	2009-10-14 21:21:58	1080
00030987185	PC	2009-10-16 21:28:03	2009-10-16 21:44:56	1008
00030987186	PC	2009-10-19 21:53:02	2009-10-19 23:37:57	1065
00030987187	PC	2009-10-21 01:18:31	2009-10-21 01:19:56	65
00030987188	PC	2009-10-26 22:39:02	2009-10-26 22:44:56	333
00030987189	PC	2009-10-28 11:27:04	2009-10-28 13:24:58	1663
00030987191	PC	2009-11-01 00:37:38	2009-11-01 00:54:56	1030

Table 3. Observation log for IGR J17544−2619.

Sequence	Instrument/Mode	Start time (UT) (yyyy-mm-dd hh:mm:ss)	End time (UT) (yyyy-mm-dd hh:mm:ss)	Net Exposure (s)
00035056083	PC	2009-02-21 16:45:15	2009-02-21 18:32:57	1387
00035056084	PC	2009-02-24 07:31:27	2009-02-24 07:50:58	1160
00035056085	PC	2009-02-28 01:28:32	2009-02-28 01:45:57	1034
00035056086	PC	2009-03-03 19:35:54	2009-03-03 21:18:57	784
00035056087	PC	2009-03-07 20:03:32	2009-03-07 21:41:56	268
00035056088	PC	2009-03-14 01:11:35	2009-03-14 01:28:56	1031
00035056089	PC	2009-03-16 15:35:47	2009-03-16 17:17:37	2126
00035056090	PC	2009-03-21 17:59:47	2009-03-21 19:40:56	1450
00035056091	PC	2009-03-28 18:37:33	2009-03-28 18:53:56	946
00035056092	PC	2009-03-31 14:11:09	2009-03-31 14:15:57	281
00035056093	PC	2009-04-04 17:56:02	2009-04-04 18:02:56	410
00035056094	PC	2009-04-07 00:20:07	2009-04-07 00:39:57	916
00035056095	PC	2009-04-11 10:30:29	2009-04-11 12:14:58	889
00035056096	PC	2009-04-18 04:35:54	2009-04-18 04:38:57	163
00035056097	PC	2009-04-25 00:26:41	2009-04-25 00:42:58	698
00035056098	PC	2009-04-28 07:20:35	2009-04-28 13:42:55	2118
00035056099	PC	2009-05-02 09:02:27	2009-05-02 09:18:57	968
00035056100	PC	2009-05-05 01:31:22	2009-05-05 03:12:57	962
00035056101	PC	2009-05-09 04:42:29	2009-05-09 06:27:56	1237
00035056102	PC	2009-05-16 02:35:27	2009-05-16 04:25:57	865
00035056103	PC	2009-05-19 17:21:57	2009-05-19 19:03:57	879
00035056104	PC	2009-05-23 09:28:09	2009-05-23 11:16:57	1361
00035056105	PC	2009-05-24 22:29:23	2009-05-25 00:15:56	959
00035056106	PC	2009-05-25 14:29:38	2009-05-26 06:27:56	565
00035056107	PC	2009-05-30 23:00:07	2009-05-30 23:08:56	519
00035056108	PC	2009-06-02 07:23:10	2009-06-02 09:02:56	400
00035056110	PC	2009-06-06 04:32:43	2009-06-06 09:08:57	332
00354221000	BAT/evt	2009-06-06 07:45:04	2009-06-06 08:05:06	1202
00354221000	WT	2009-06-06 07:51:53	2009-06-06 07:56:29	276
00354221000	PC	2009-06-06 07:56:31	2009-06-06 07:58:01	90
00354221001	PC	2009-06-06 08:58:36	2009-06-06 09:05:57	417
00035056109	PC	2009-06-06 09:20:02	2009-06-06 11:09:57	776
00035056111	PC	2009-06-06 15:17:45	2009-06-06 20:48:54	4409
00035056112	PC	2009-06-10 17:43:17	2009-06-10 19:30:57	1376
00035056113	PC	2009-06-13 09:44:23	2009-06-13 11:29:58	1016
00035056114	PC	2009-06-16 18:24:52	2009-06-16 18:27:57	143
00035056115	PC	2009-06-20 02:36:19	2009-06-20 07:39:57	1551
00035056116	PC	2009-06-23 18:36:44	2009-06-23 18:55:59	1060
00035056117	PC	2009-06-26 06:14:29	2009-06-26 06:27:09	745
00035056118	PC	2009-06-30 16:19:39	2009-06-30 16:44:56	1510
00035056119	PC	2009-07-01 13:01:11	2009-07-01 14:50:56	1511
00035056120	PC	2009-07-03 19:56:46	2009-07-03 21:50:57	2051
00035056121	PC	2009-07-07 23:35:35	2009-07-07 23:46:57	672
00035056122	PC	2009-07-11 15:57:25	2009-07-11 19:21:57	2141
00035056124	PC	2009-07-17 08:32:07	2009-07-17 10:16:56	1063
00035056125	PC	2009-07-21 00:54:22	2009-07-21 02:06:57	1068
00035056126	PC	2009-07-25 18:35:12	2009-07-25 18:54:56	1165
00035056127	PC	2009-07-28 12:15:35	2009-07-28 12:30:18	864
00035056128	PC	2009-07-31 03:18:44	2009-07-31 03:31:56	783
00035056129	PC	2009-08-04 19:30:26	2009-08-04 19:46:56	943
00035056131	PC	2009-08-11 23:13:57	2009-08-11 23:29:58	944
00035056132	PC	2009-08-22 22:43:53	2009-08-22 22:56:58	761
00035056134	PC	2009-09-05 05:00:41	2009-09-05 05:17:57	1016
00035056135	PC	2009-09-12 11:46:59	2009-09-12 12:07:57	1251
00035056136	PC	2009-09-19 23:40:40	2009-09-19 23:59:56	1146
00035056137	PC	2009-09-22 01:27:14	2009-09-22 03:16:58	1331
00035056138	PC	2009-09-29 13:29:21	2009-09-29 16:51:57	1563
00035056139	PC	2009-09-30 20:26:37	2009-09-30 23:43:58	947

Table 3. Observation log for IGR J17544−2619. Continued.

Sequence	Instrument/Mode	Start time (UT) (yyyy-mm-dd hh:mm:ss)	End time (UT) (yyyy-mm-dd hh:mm:ss)	Net Exposure (s)
00035056141	PC	2009-10-06 06:04:55	2009-10-06 06:22:58	1070
00035056142	PC	2009-10-10 05:01:15	2009-10-10 06:50:57	1571
00035056143	PC	2009-10-13 01:56:47	2009-10-13 02:23:56	1607
00035056144	PC	2009-10-17 23:09:57	2009-10-17 23:31:56	1316
00035056146	PC	2009-10-27 03:18:01	2009-10-27 03:33:56	942
00035056147	PC	2009-10-31 05:12:03	2009-10-31 05:30:57	1113
00035056148	PC	2009-11-03 10:29:20	2009-11-03 10:46:58	1058